Performance Assessment of an S-band Return Link for Messaging and Mobile Interactive Broadcasting

Romain Hermenier
German Aerospace Center (DLR), Institut of Communication and Navigation
Oberpfaffenhofen D-82234 Wessling, +49 8153 28-3138, romain.hermenier@dlr.de

Sandro Scalise
German Aerospace Center (DLR), Institut of Communication and Navigation
Oberpfaffenhofen D-82234 Wessling, +49 8153 28-2856, sandro.scalise@dlr.de

Abstract

Within this paper we examine the performance in terms of aggregate MAC throughput of the return link of a messaging and mobile interactive broadcast system in S-band. More specifically, an analysis is done to investigate the impact of using two different air interfaces (synchronous and asynchronous access) within the same bandwidth on the instantaneous MAC throughput within one beam. All considerations take into account a realistic population density as well as the propagation envrionment and a linguistic pattern over Europe.

1. Introduction

Nowadays Mobile Satellite Services (MSS) are experiencing a new momentum thanks to the success of satellite-based broadcast to mobile receivers like XM-Radio and Sirius. These two systems are based on a hybrid terrestrial and space infrastructure which allow them to offer a substantial number of radio and video channels through very small and transportable receivers. New bidirectional systems (such as Terrestar or W2A) exploiting the new S-band licensing rule based on the principle of Ancillary Terrestrial Component (ATC) in United States of America or Complementary Ground Component (CGC) in Europe (hybrid satellite/terrestrial network) are currently under development.

The interactive broadcast system considered in this paper is described in [1] and corresponds to a suitable integrated communications system capable of efficiently use the available S-band allocation for pan-European MSS (15 MHz in both uplink and downlink for each of the two licensed operators) to provide three main classes of services, hereafter referred to as Service Segments (SS), namely: SS1 (Interactive mobile broadcast services), SS2 (Messaging services for handhelds and vehicular terminals) and SS3 (Real-time emergency services such as voice and file transfer, mainly addressing institutional users on-the-move such as fire brigades, civil protections, etc…)

The focus of this work is on the return link where two types of radio interfaces are envisaged in this system. The first one is based on Enhanced Spread Spectrum Aloha (E-SSA) for SS1 and SS2 ([2], [3], [4]) whereas the other one based on Quasi-Synchronous Code Division Multiple Access (QS-CDMA) Demand Assignment Multiple Access (DAMA) scheme [5] is used for SS3. We remind to [2], [3] and [4] for detailed insights about E-SSA and to [5] for QS-CDMA.

Furthermore E-SSA and QS-CDMA share the same bandwidth which poses the problem of the Multiple Access Interference (MAI) generated by QS-CDMA terminals over E-SSA ones and other way around. We will cope later with this issue in this paper. We refer to [1] for more details about the coexistence of synchronous (QS-CDMA) and asynchronous (E-SSA) access in this system.

The goal of this paper is therefore to assess the performance of the system in terms of MAC throughput. Whereas the second section focuses on the system model, the third section provides an overview of the interferences model developed within this work. Finally the different scenarios as well as the simulation results are presented in the last section.

2. System Model

2.1. Space Segment Model

The system relies on a bidirectional satellite component as well as on CGCs. Whereas the satellite component can be used by all three service segments, the terrestrial component will only be used by SS1 and SS2 [1].

The spot beam coverage of the system is simulated using a database which contains a grid with antenna gain values per coordinate for the area of interest (Europe). It corresponds to linguistic beam coverage over Europe as displayed in Fig.1. The satellite position is 10°W. This coverage includes 6 beams over Europe. The numbering of these beams is done as follows: Beam 1: Germany, Beam 2: France, Beam 3: Italy, Beam 4: Poland, Beam 5: Spain, Beam 6: United Kingdom. Moreover a frequency reuse factor of 3 is used with the following pattern: Beams 1 (Germany) and 5 (Spain) use the same frequency, Beams 2 (France) and 4 (Poland) use the same frequency, Beams 3 (Italy) and 6 (United Kingdom) use the same frequency.

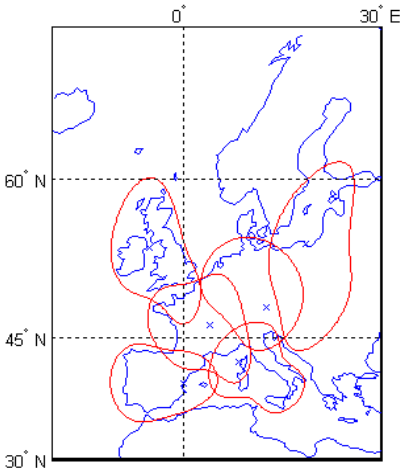

Figure 1: Linguistic beam coverage over Europe

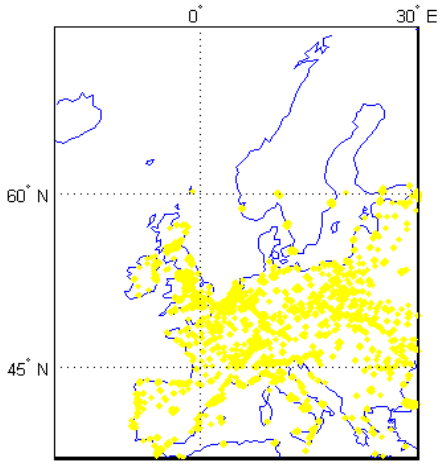

Figure 2: Distribution of 10,000 users over Europe

2.2. Users' Distribution Model

The users' distribution model has been developed using different realistic databases presented hereafter. It specifies information on the position of each user as well as on the beam each user will use to transmit.

A) Database on Population Density: A topographic database is used within this work. It provides the spatial distribution of human population across the globe. Population densities are available from the Gridded Population of the World project [6]. These data are available in a 2.5' grid for all continents and correspond to the population density in year 2000. A defined number of users is given as input parameter and then distributed over Europe according to the population density as can be seen in Fig.2.

B) Database on Propagation Environment: Depending on his position, each user will be subjected to a different propagation state, which can go from Line-of-Sight (LOS) with the satellite until complete blockage. This database on propagation zone is provided by the Global Land Cover Facility [7]. It offers a classification of geographical areas with a grid step equal 0.00833 degree for both the longitude and latitude and it considers 14 types of land cover classes as shown in Table 1. Fig.3 displays the propagation environment over Europe. Thanks to this database and the users' position, the land cover class of each user can be determined.

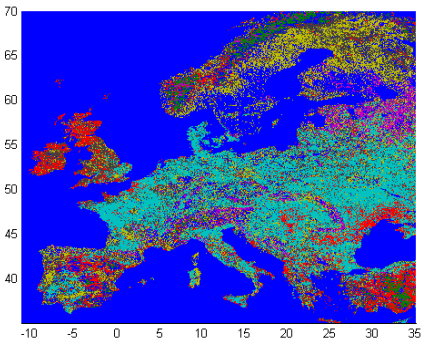

Figure 3: Propagation environment over Europe

Land cover classes		LMS acc. to [8]
0	Water	NA
1	Evergreen Needleleaf Forest	HTS
2	Evergreen Broadleaf Forest	HTS
3	Deciduous Needleleaf Forest	HTS
4	Deciduous Broadleaf Forest	HTS
5	Mixed Forest	HTS
6	Woodland	ITS
7	Wooded Grassland	ITS
8	Closed Shrubland	OPE
9	Open Shrubland	OPE
10	Grassland	OPE
11	Cropland	OPE
12	Bare Ground	OPE
13	Urban and Built-up	SUB

Table 1: Correspondance between land cover classes and land mobile satellite (LMS) channels

However the focus is only on the users in LOS with the satellite. [8] provides 3 states models for several environments and elevation angles in which the percentage of time in LOS conditions can be estimated. The model kept for this work contains four different environment types namely Open area (OPE), Suburban area (SUB), Intermediate Tree Shadowing (ITS) and Heavy Tree Shadowing (HTS). Moreover the 3 states are defined as follows: state 1 is considered as LOS conditions, state 2 as light shadow and state 3 as heavy shadow. In Table 2 is displayed the percentage of time in each state depending on the environment types for a 40 degrees elevation angle.

Environment type	% time state 1	% time state 2	% time state 3
OPE	50	37.5	12.5
SUB	45.4	45.4	9.2
ITS	39.3	35.7	25
HTS	0	50	50

Table 2: Time share of the Markov chain states for 40 degrees satellite elevation

Following the LOS share defined in Table 2 and the mapping of the environment types with the land cover classes given in Table 1 an estimation of the users in LOS has been performed as follows: users with land cover classes between 0 and 5 are discarded, 60.7% of users with land cover classes between 6 and 7 are randomly discarded, 50% of users with land cover classes between 8 and 12 are randomly discarded and 54.6% of users with land cover class 13 are randomly discarded. For the rest of this paper, when speaking about “users” we refer to the users in LOS with the satellite.

Another issue to solve was the selection of the beam each user will use to transmit. Indeed as can be seen in Fig.1 the neighboring beams overlap and hence users can be covered by more than one beam. Because of this it has been decided that if a user is in the overlap area, he will use the beam for which he has the highest forward link Signal-to-Noise Ratio (SNR). Since the fading is affecting both beams in the same way, such decision has been taken over the nominal (LOS) link budget. Thus this allows us to know the maximal number of users per beam given the overall number of LOS users defined in the previous section.

2.3. Air Interface Configuration

The typical configuration for E-SSA and QS-CDMA radio interfaces are given in [1]. However within this paper the following configuration has been investigated: E-SSA with a terminal Equivalent Isotropically Radiated Power (EIRP) of 2 dBW (packet size of 600 bits, data rate of 5 kbps and spreading factor of 256), E-SSA with a terminal EIRP of 5 dBW (packet size of 600 bits, data rate of 10 kbps and spreading factor of 128) and QS-CDMA with a terminal EIRP of 11 dBW or 15 dBW (data rate from 8 up to 512 kbps and spreading factor of 8, 16, 32, 64, 128 or 256).

3. Interferences Model

This section explains the packet interferences model developed to simulate the mutual interferences between E-SSA bursts and the interference between E-SSA bursts and QS-CDMA packets. The steps detailed next are performed beam by beam. For a better understanding we are going to take as example the first beam (Germany), though the same methodology is applicable for all the other beams. The beam interfering with Germany is the beam over Spain. For the rest of this paper when speaking about a “burst” (or packet) it means that this “burst” (or packet) is emitted from a terminal located in Germany. When speaking about “interfering bursts” (or “interfering packet”) we refer here to the users located in Spain and interfering with the ones in Germany since they reuse the same frequency.

The principle of the model is the following: assuming a constant burst length, a burst B2 will interfere with a burst B1 if the transmission starting time of B2 is comprised between [-TxB1, TxB1] where TxB1 represents the transmission time of B1. Fig.4 displays an example where 7 bursts are present. It shows how all the bursts interfere with the burst B1. The transmission starting time of each of the 7 bursts has been chosen randomly.

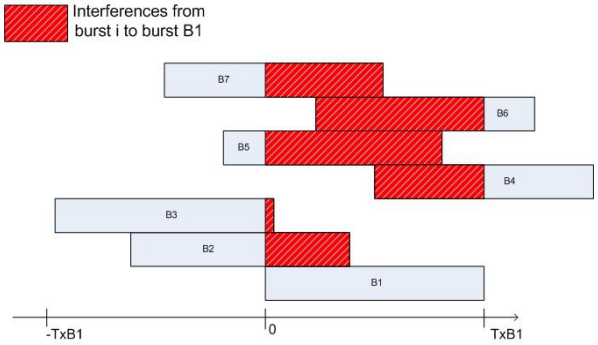

Figure 4: Interferences affecting the burst B1.

Considering that each user transmits one burst at a specific time instant, the transmission starting time of each user can be simulated using a random variable uniformly distributed in [-TxB1, TxB1] which becomes [-1, 1] after normalization. And thus the percentage of interference between the bursts can be computed.

This simplified approach not including a time component results in an average interference level reduced by 50%. However due to the three different services considered in the system, bursts and packets can have variable length. Here are the ones used in this model: transmission time of a QS-CDMA packet: 96 ms [1], transmission time of an E-SSA burst with a 2 dBW terminal EIRP: 120 ms (considering a length of 600 bits at 5 kbps) and transmission time of an E-SSA burst with a 5 dBW terminal EIRP: 60 ms (considering a length of 600 bits at 10 kbps)

The E-SSA bursts with a 2 dBW terminal EIRP have the longest transmission time; the normalization is therefore done taking this transmission time as reference. The transmission starting time of these bursts will be uniformly distributed in [-1, 1]. Regarding E-SSA bursts with a 5 dBW terminal EIRP, their transmission time is half than the previous one. The transmission starting time of these packets will therefore be uniformly distributed in [-0.5, 0.5]. Finally QS-CDMA packets are, without loss of generality, fixed and centered in 0 since QS-CDMA packets are continuously transmitted. For a better understanding, an example of burst distribution where 2 QS-CDMA packets, 3 E-SSA bursts with a 2 dBW terminal EIRP, and 3 E-SSA bursts with a 5 dBW terminal EIRP are considered is displayed in Fig.5.

QS-CDMA packets do not interfere among each other since they are assumed here being mutually orthogonal. Still there might be some interference coming from users located in the beam reusing the same frequency. This interference is currently not considered, since it is seen as a “second order” effect, also because the number of QS-CDMA users in the adjacent beam can significantly differ (QS-CDMA might even not be used in such beam). Moreover, if the two beams are served by the same hub and the overall number of QS-CDMA users is low, some kind of coordination in the spreading code assignment could be envisaged. Thus, we only considered the interferences of QS-CDMA users located in both beams (useful and interfering one) towards E-SSA users. Regarding E-SSA, the bursts are transmitted asynchronously, thus generating mutual interference as well as interference to QS-CDMA carriers.

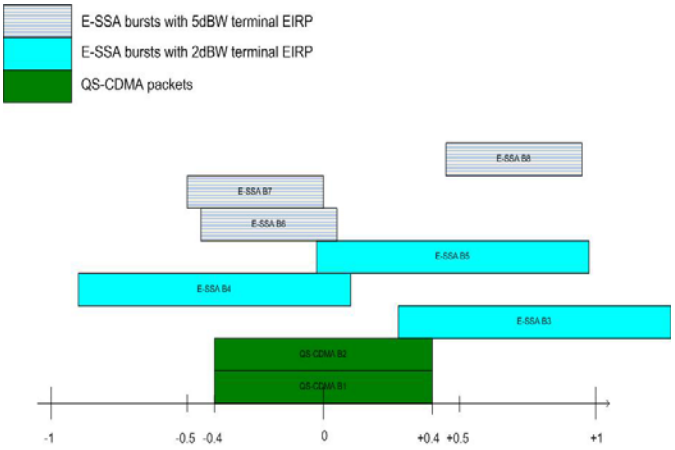

Figure 5: Distribution of 7 bursts according to the packets interferences model

Thanks to this model, whatever the air interface (E-SSA or QS-CDMA) the percentage of interference affecting one burst or packet can be estimated. In summary, for each E-SSA burst is computed on the hand the aggregate interference from all the other E-SSA bursts or QS-CDMA packets located in the same beam as the considered burst (Germany), assuming that the latter are cancelled with a given efficiency, and on the other hand the aggregate interference from all the E-SSA bursts or QS-CDMA packets located in the interfering beam (Spain), assuming that the latter are cancelled with a given efficiency.

Regarding QS-CDMA packet is computed the aggregate interference from all the other E-SSA bursts located in the same beam as the considered packet (Germany) as well as the aggregate interference from all the E-SSA bursts located in the interfering beam (Spain).

A) Noise Rise Computation for QS-CDMA users: For QS-CDMA, there is no MAI due to other QS-CDMA carriers since they are orthogonal (residual MAI due to non ideal orthogonality is assumed to be compensated through the link margin and not considered here as already explained). The MAI due to E-SSA can be modeled as an increase in the noise level (Noise Rise) according to formula 1.

(1) $NR^{QS-CDMA} = 1 + \sum_{j=1}^{N_u^{E-SSA}} \frac{E_c^{(j)}}{N_0} \alpha(j)$ where $\alpha(j)$ represents the percentage of interference of E-SSA burst j to the considered QS-CDMA burst, as defined in the previous sub-section. N_u^{E-SSA} is the total number of E-SSA users located in Germany and Spain (interfering beam). In order to calculate the Noise Rise affecting the QS-CDMA users, the $\frac{C^{E-SSA}}{N}$ up (uplink SNR for each E-SSA user) must be first computed.

Moreover, it shall be taken into account that closed-loop power control is used in QS-CDMA. To model this closed-loop power control an inverse link budget is performed to determine the nominal EIRP for each QS-CDMA carrier which would guarantee the required SNR at the hub. A lognormal fluctuation of C with standard deviation equal to 0.35 dB is added to take into account power control errors. In order to avoid using more power than the maximal EIRP (11 dBW or 15 dBW), the final EIRP for QS-CDMA users is defined as displayed in formula 2.

(2) $EIRP^{QS-CDMA} = \min(EIRP_{\max}^{QS\_CDMA}, EIRP_{nom}^{QS-CDMA} + C)$

Knowing the final EIRP as well as the Noise Rise affecting the QS-CDMA users a link budget can be performed. To check if a QS-CDMA user closes the link budget or not, in other words if the packets can be decoded, different spreading factor can be used namely: 8, 16, 32, 64, 128 and 256. We check first with the lowest spreading factor (highest data rate). If the packet can not be decoded, a higher spreading factor is selected. If the link budget can not be closed for spreading factor 256 (lowest data rate), the QS-CDMA user can not transmit. QS-CDMA packets are decoded following the Packet Error

Rate (PER) vs. $\frac{E_b}{N_0}$ curve in [1]. If the resulting $\frac{E_b}{N_t}$ is below 0.5 dB the burst is not decoded (PER=1), whereas if it is higher than 2 dB, PER=0 and the burst is always decoded. For intermediate values of $\frac{E_b}{N_t}$, a linear interpolation is performed to get the corresponding PER.

B) Noise Rise Computation for E-SSA users: Regarding E-SSA users, on the one hand Interference Cancelation (IC) is used by the QS-CDMA demodulator to eliminate the QS-CDMA carriers and on the other hand Successive Interference Cancelation (SIC) is applied to recover the E-SSA bursts. The Noise Rise calculation is therefore a bit more complex. There is a fixed part due to the residual power after cancellation of the QS-CDMA carriers performed by the QS-CDMA demodulator and a variable part which is decreasing as long as the SIC progresses within the E-SSA demodulator. In formulas:

(3) $NR_k^{E-SSA} = 1 + (1-\eta_{IC}) \sum_{i=1}^{N_u^{QS-CDMA}} \frac{E_C^{(i)}}{N_0} + (1-\eta_{SIC}) \sum_{j=1}^{A(k)} \frac{E_C^{(j)}}{N_0} \alpha_1(j) + \sum_{j=1}^{B(k)} \frac{E_C^{(i)}}{N_0} \alpha_2(j)$ where A(k) represents the number of E-SSA bursts which at iteration k of the SIC has been already decoded, B(k) represents the number of E-SSA bursts which at iteration k of the SIC has not been decoded yet, (A(k) + B(k) shall be always equal to $N_u^{E-SSA} - 1$, taking into account the E-SSA bursts which is being decoded at iteration k, namely the one with the highest received $\frac{E_b}{N_t}$ among those not being decoded yet, with N_u^{E-SSA} being the number of E-SSA users considered inside one beam plus those inside the interfering beam), $\alpha_1(j)$ is the percentage of interference between the burst A(j) and the E-SSA burst considered, $\alpha_2(j)$ is the percentage of interference between the burst B(j) and the E-SSA burst considered, $N_u^{QS-CDMA}$ the total number of QS-CDMA users located in Germany and Spain (interfering beam), η_{IC} and η_{SIC} : efficiencies of IC and SIC, respectively.

For E-SSA terminals, a simple open-loop power control scheme is in place. The EIRP value of each E-SSA terminal is given by formula 4.

(4) $EIRP^{E-SSA} = \min(EIRP_{\max}^{E-SSA}, L + N_{SAT} + K - R_{rand})$

As for QS-CDMA, the minimum between the maximal EIRP (2 dBW or 5 dBW) and the variable EIRP is chosen to avoid exceeding the EIRP terminal capability. In formula 4, L represents the path loss in dB estimated through the received signal in the forward link. A lognormal random fluctuation with standard deviation equal to 1 dB for OPE environment and to 2 dB for ITS and SUB environments (see Table 2) is added to take into account estimation errors. N_{SAT} is the noise + interference power level at the satellite receiver, K is a constant equal to $\frac{C}{N_0 + I_{0\,t}} - G_S$, where $\frac{C}{N_0 + I_{0\,t}}$ is the target value used for the desired Signal-to-Noise Interference Ratio (SNIR) at the satellite transponder input and G_S is the satellite antenna gain. R_{rand} is an optional additional power randomisation uniformly distributed between 0 and $R_{\max}$. The parameters N_{SAT}, K and $R_{\max}$ are distributed through the forward link signalling and supposed to be available at the terminal.

Knowing the final EIRP as well as the Noise Rise affecting the E-SSA users, a link budget is performed on the return link for each main user using E-SSA. At the first iteration the burst with the highest SNR is selected. E-SSA bursts are decoded following the Frame Error Rate (FER) vs. $\frac{E_b}{N_0}$

[1]. If $\frac{E_b}{N_t}$ is below 1 dB the burst is not decoded (FER=1), whereas if $\frac{E_b}{N_t}$ is higher than 4.5dB, FER=0 and the burst is always decoded. For intermediate values of $\frac{E_b}{N_t}$, a linear interpolation is performed to get the corresponding FER. If the burst with the highest SNR has been decoded successfully the process is reiterated and the noise rise for the remaining bursts is recomputed according to formula 3. At the second iteration we try to decode the burst having the next highest SNR. However if the first burst has not been decoded, none of the following bursts will be decoded since SIC is used. To decode an E-SSA burst two spreading factors are used, namely: 128 if the E-SSA user has a 5 dBW terminal EIRP or 256 for E-SSA users having a 2 dBW terminal EIRP. Knowing the spreading factors of all the main users (E-SSA and QS-CDMA) the performance of the system can be assessed in terms of MAC throughput per beam and per transmission technique.

4. Selected Scenarios and Simulation Results

To evaluate the end-to-end performance of the system, different scenarios have been defined in which the MAC throughput vs. the offered traffic (in Pkts/s) is given as output. In a first step, four scenarios have been set with only E-SSA users as displayed in Table 3. Scenarios 1 and 2 (S1 and S2) only include E-SSA users with a 2 dBW terminal EIRP and 256 as spreading factor whereas scenarios 3 and 4 (S3 and S4) considered only E-SSA users with a 5 dBW terminal EIRP and 128 as spreading factor. Finally scenarios 1 and 3 will have 0 dBW for $R_{\max}$ whereas 3 dBW will be used for scenarios 2 and 4. In these four scenarios both the efficiencies of IC and SIC are set to 95%.

	S1	S2	S3	S4
E-SSA terminal EIRP (in dBW)	2	2	5	5
Data Rate (in kbps)	5	5	10	10
Available spreading factor	256	256	128	128
R_{max} (in dBW)	0	3	0	3
Number of QS-CDMA users	0	0	0	0

Table 3: Definition of E-SSA scenarios without QS-CDMA users

In a second step 10 and then 30 QS-CDMA users will be added to the best and worst scenarios to study the influence of QS-CDMA users on both the overall and E-SSA MAC throughputs. Fig.6 displays the MAC throughput in Mbit/s of the four different scenarios.

It can be noticed that in all the cases when the offered traffic (i.e. the number of users) becomes too important, the throughput collapses. The reason of this behavior is due to the interferences level which increases with the offered traffic inside each beam, i.e. with the number of users since each user transmits one burst in these scenarios. Furthermore setting up $R_{\max}$ to 3 gives us higher performances. With this parameter equals to 3 the EIRP of the different users are in average lower and therefore less interferences are produced.

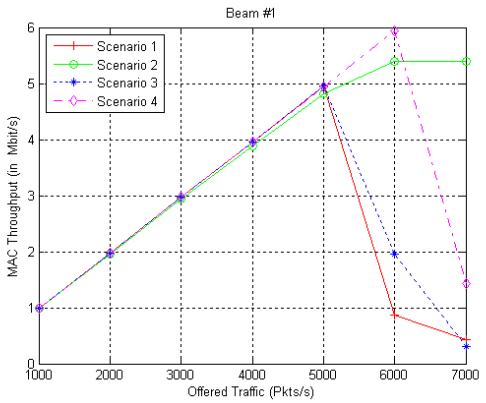

Figure 6: MAC throughput for scenarios 1, 2, 3 and 4.

The main difference among the four scenarios is in the number of users considered within the beam. For the same offered traffic, scenarios 1 and 2 allow twice more users to transmit than for scenarios 3 and 4. The data rate of the two first scenarios is indeed 5 kbps whereas for scenarios 3 and 4 the data rate is about 10 kbps. From this point of view the best performances are achieved in scenario 2, whereas scenario 3 has the lowest throughput. Thus 10 and then 30 QS-CDMA users are added to these two scenarios.The new aggregate MAC throughput is depicted in Fig 7. Focusing on the E-SSA users, Fig. 8 displays the MAC throughput of E-SSA users only.

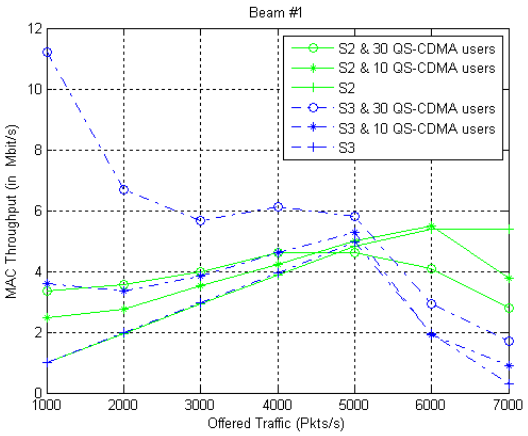

Figure 7: Aggregate MAC throughput for 0/10/30 QS-CDMA users for scenarios 2 and 3.

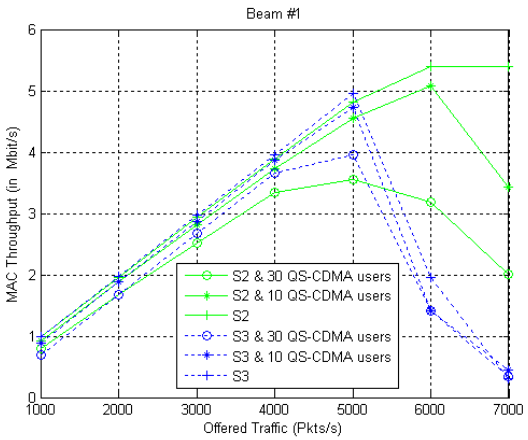

Figure 8: E-SSA MAC throughput for 0/10/30 QS-CDMA users for scenarios 2 and 3.

Results show that in scenario 3, the E-SSA performance are mainly limited by the self interference because of the lower spreading factor and of the insufficient power unbalance, hence the presence of up to 30 QS-CDMA carriers causes a marginal degradation. In turn, for scenario 2, where E-SSA operates at higher efficiency, a significant degradation in the E-SSA MAC throughput can be detected for more than 10 QS-CDMA carriers.

5. Conclusion

In this work, an estimation of the MAC throughput of the interactive broadcast system defined in [1] has been investigated. Realistic data such as the population density and the land cover classes have been taken into consideration to set up our environment. Furthermore an interferences model has also been developed to simulate the impact of the E-SSA bursts and QS-CDMA packets among each other.The results show that the performance of the system is mainly limited by the self interference and the number of QS-CDMA carriers per beam. Focusing on the E-SSA air interfaces, a trade-off must be carried out, depending on the desired needs, between the targeted number of users for the system and the configuration of the E-SSA air interface. Moreover, as expected, a major role is played by the power control mechanism, since the SIC in the E-SSA demodulator relies on the presence of a certain level of power unbalance. These results have confirmed that the proper dimensioning of the open loop power control is a crucial point in order to reach the theoretical MAC throughput performance.

References

[1] S. Scalise et al, “System design for pan-european mss services in s-band,” in 5th Advanced Satellite Multimedia Systems Conference (ASMS), Sep. 2010.
[2] O. Del Rio Herrero et al, “A high efficiency multiple access scheme for machine-to-machine communications in a land mobile satellite channel,” submitted to IEEE Transactions on Vehicular Technology.
[3] ——, “Methods, apparatuses and system for asynchronous spreadspectrum communication,” European Patent Application nr. 08290801.3, Aug. 2008.
[4] ——, “A high efficiency scheme for quasi-real-time satellite mobile messaging systems,” in 10th Signal Processing for Space Communications, Oct. 2008.
[5] R. De Gaudenzi et al, “Bandlimited quasi-synchronous cdma: A novel satellite access technique for mobile and personal communications systems,” IEEE Journal in Selected Areas in Communications, vol. 10, no. 2, pp. 328–343, Feb. 1992.
[6] Gridded population of the world. [Online]. Available: http://sedac.ciesin. columbia.edu/gpw/index.jsp
[7] Global land cover facility. [Online]. Available: http://glcf.umiacs.umd. edu/index.shtml
[8] F. Pérez-Fontan et al, “S-band LMS propagation channel behaviour for different environments, degrees of shadowing and elevation angles,” IEEE Transactions on Broadcasting, vol. 44, no. 1, pp. 40–76, Mar. 1998.